The International Archives of the Photogrammetry, Remote Sensing and Spatial Information Sciences, Volume XLVIII-1/W2-2023
ISPRS Geospatial Week 2023, 2–7 September 2023, Cairo, Egypt

BENCHMARKING COLLABORATIVE POSITIONING AND NAVIGATION BETWEEN GROUND AND UAS PLATFORMS

A. Masiero[1], L. Morelli[2,3], C. Toth[4], F. Remondino[2]

[1] University of Florence, Florence, Italy – Email: andrea.masiero@unifi.it

[2] 3D Optical Metrology (3DOM) unit, Bruno Kessler Foundation (FBK), Trento, Italy – Email: <lmorelli><remondino>@fbk.eu

[3] Dept. of Civil, Environmental and Mechanical Engineering (DICAM), University of Trento, Italy

[4] The Ohio State University, Columbus, Ohio, USA – Email: toth.2@osu.edu

Commission II

KEY WORDS: collaborative positioning, UWB, vision, LiDAR, UAS, Kalman filter, GNSS, SLAM

ABSTRACT:

The availability of Global Positioning System (GPS), or more in general of Global Navigation Satellite Systems (GNSS), and the development of smart mobile devices, able to exploit the geospatial information provided by GPS/GNSS and integrate their use within many applications, have had a dramatic impact on the everyday life of most of the World population. While GNSS allows for real-time positioning in a wide range of scenarios, there are many challenging environments, such as tunnels and urban canyons, where GNSS-based solutions are inaccurate, unreliable, or even unavailable. The enormous interest in applications requiring ubiquitous positioning (e.g., self-driving vehicles) has been motivating the development of alternative positioning systems to support or substitute GNSS when operating in challenging scenarios. Alternative positioning systems to GNSS are usually developed by employing several sensors, such as radio-based, vision, LiDAR (Light Detection and Ranging), and RADAR (Radio Detection and Ranging). Furthermore, a collaborative approach can also be developed to increase the robustness of the navigation solution of inter-connected vehicles. To support research in this area, we are presenting the CONTEST (Collaborative pOsitioning and NavigaTion bEtween ground and uaS plaTforms) dataset, aiming at providing multiple data streams to test collaborative positioning approaches, involving both terrestrial and aerial platforms, based on the use of several sensors, such as Ultra-Wide Band (UWB) transceivers, cameras, LiDARs, GNSS. Data are described and some initial results presented.

1. INTRODUCTION

Recently, we have witnessed rapid developments of positioning solutions and their applications, such as GNSS (Global Navigation satellite System), autonomous vehicle (AV) and Unmanned Aerial Systems (UAS) technologies. This is calling for appropriate solutions to ensure safe and reliable positioning and navigation of such autonomous platforms in any operational environment and condition, including situations where air and ground platforms share the same space or when GNSS is not available.

GNSS allows positioning and navigation of ground and aerial platforms almost everywhere and has been widely used in a large variety of devices and applications, including mapping. But, despite developments in hardware technologies and Radio-Frequency (RF) signal processing, GNSS cannot be available or reliable in certain environments, such as dense forestry, tunnels, urban canyons or when RF interference is present (Humphreys, 2017), such as spoofing or jamming (Ruegamer and Kowalewski, 2015; Zidan et al., 2016).

Therefore, alternative positioning approaches have been studied (Raquet, 2013; Schmidt, 2015; Grejner-Brzezinska et al., 2016; Vitan et al., 2018; Liang et al., 2022). One of the applicable techniques is the use of collaborative navigation (CN), where platforms (often called agents) navigating in close vicinity can share position and navigation information (vehicle-to-infrastructure - V2I and vehicle-to-vehicle - V2V communications) and a joint navigation solution can potentially provide better results for all platforms with respect to individual ones (Mu et al., 2011; Kealy et al., 2016; Fan et al., 2019; Pascacio et al., 2021; Icking and Schon, 2022).

As vehicles are normally equipped with multiple instruments, on-board sensors are often used to create an integrated system or a sensor network, shown in Fig. 1. This can (i) compensate for the unreliability of GNSS when necessary and (ii) ensure safety by detecting vehicles, people and other objects in the neighbourhood area in real-time.

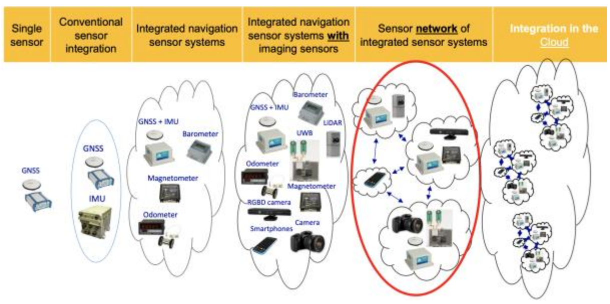

Figure 1: Convergence in sensor integration approaches.

Vision has already been extensively used for positioning purposes; for instance, in real-time SLAM (Simultaneous Localization and Mapping) or VO (Visual Odometry) approaches as well as offline SfM (Structure from Motion) methods to reconstruct the object space, including sensor trajectory recovery from overlapping image sequences (Taketomi et al., 2017; Zou et al., 2019; Menna et al., 2022). Thanks to major advancements in data analytics, particularly in deep learning, detecting objects and people has become feasible and already widely used in practice. Given the affordable cost of cameras and the huge amount of information acquired, vision is ideal to support a variety of object recognition and positioning tasks, including collision avoidance, scene labeling, relative and absolute positioning, object tracking, etc. Information obtained from these processing steps, such as distance (if scale is known) and view angles of an object with respect to the platform can support collaborative navigation (Masiero et al., 2021), as besides this data, only inter-platform communication is needed.

Similarly to GNSS, cameras may not be effective in all environments; for instance, in low light conditions, blinded by the sun, strong shadows, inclement weather, featureless environments, repetitive patterns, etc. For this reason, LiDAR (Light Detection and Ranging) as well as Ultra-Wide-Band (UWB) ranging sensors (Gabela et al., 2019) and, if available, odometers from the vehicle (e.g., wheel odometers) or step sensor of wearable devices are considered good alternatives (or complementary) to cameras for positioning purposes by exploiting LiDAR odometry, UWB trilateration. etc.

1.1 Paper objective

The provision of GNSS-based alternative and complementary positioning solutions has been of high interest for a long while (Bonenberg et al., 2023). Since reliable GNSS signal reception cannot be guaranteed in urban and vegetated areas as well as when signals are subject to unintentional and intentional interferences, collaborative positioning solutions are of high interest. Urged by this new R&D need, the goal of the work is twofold:

- to present the *CONTEST* (Collaborative pOsitioning and NavigaTion bEtween ground and uaS plaTforms) dataset to support the development, testing and comparison of the individual or integrated use of imaging data, LiDAR and UWB ranging for collaborative positioning and navigation purposes, including the possibility to execute and validate visual and LiDAR odometry or SLAM approaches, hybrid adjustment and UWB trilateration algorithms, etc. To ensure reliable validation results, accurate GNSS-based reference solutions are provided for all the platforms.
- to report initial results achieved with the *CONTEST* dataset and open the scene to further analyses and performance validation. A unique aspect of the dataset is that, for the first time, various observations in a 3D environment are provided, allowing the combination of ground (connected vehicles) and air (swarm of drones) platforms for collaborative navigation approaches.

2. COLLABORATIVE NAVIGATION

The concept of collaborative navigation (CN) represents the next level of generalization of sensor integration by integrating sensors deployed on multiple platforms (Lee et al., 2012; Buehrer et al., 2018). The two fundamental conditions of CN are the availability of inter-platform range and/or angular measurements and then communication to allow data sharing in real-time.
There are several variations of the concept as well as their implementations. In general, the key idea is that the platforms (i.e., nodes or agents) form a geodetic network and, using the inter-platform measurements, the relative positions can be estimated. Therefore, a platform can be positioned in an arbitrary local coordinate system based on the observations of other platforms in the same scene. The strength of the geometry of the network can be exploited in several ways, such as distributing accurate position information to nodes that have no GNSS data, detecting anomalies of individual node navigation solutions (Wang et al., 2022) or degraded range measurements, e.g., non-line-of-sight (Wang and Jiang, 2021).
A basic CN solution uses only inter-nodal range measurements either with or without other sensor data. In the former case, the ranges are used in the navigation filters, providing additional constraints. In the second case, the ranges are used to create the geodetic network (Ladai and Toth, 2022) and then the relative position information can be used as input to the individual or joint (federated) navigation filter. The main methods to solve this problem include:

- Static geodetic approaches, such as ordinary least squares (OLS), weighted least squares (WLS), etc.
- Sequential estimators, such as conventional navigation filters (extended Kalman filters, particle filters, multiple mode filters, etc.), batch approaches (least squares “fitting” methods, solvers, SLAM, etc.).

3. THE *CONTEST* DATASET

3.1 Set-up and platforms

For field testing, an area of approximately 50 m × 50 m was chosen at the Ohio State University West Campus, see Fig.2a. The data acquisition platforms and sensors, shown in Fig. 2c-d included: static and mobile UWB transceivers, cameras, LiDARs, GNSSs and IMUs. The moving platforms included : UASs (4), vehicles (4), cyclists (2), and pedestrians (2), see Fig. 2b. The two cyclists and two pedestrians wore bicycle helmets, which had a Topcon GNSS receiver and a Pozyx UWB transceiver attached, as shown in Fig 2c. The vehicles carried multiple sensors, see the CyberCar in Fig.2d whereas the UASs used their built-in cameras). 13 precisely surveyed targets were deployed on the ground to provide ground control for the imagery. 12 UWB transceivers (anchors) were mounted on tripods over the targets, see Fig. 3a.
The setup and data acquisition lasted 8 days between 8-16 May 2022 and included deployment and surveying of ground targets, setting up UWB networks, ground vehicle data collection sessions, UAS rehearsal flights, combined ground/air data acquisitions and a few repeat tests.

Figure 2: The field test OSU campus area for the *CONTEST* data collection (a). Moving agents (cyclists, pedestrians and vehicles; flying UAS not visible) and static anchors on tripods (b). GNSS receiver and UWB transmitter installed on a helmet (c). Sensors installed on top of a vehicle (d).

https://doi.org/10.5194/isprs-archives-XLVIII-1-W2-2023-1127-2023

Static Infrastructure	**Sensor**	**Collected Data**	**Shared Data**
	12 UWB Pozyx	-	reference positions
	LiDAR: Velodyne VLP16	raw profiles	raw profiles with timestamp
Agents	**“Onboard” Sensor**	**Collected Data**	**Shared Data**
UAS1 (DJI Phantom 4Pro RTK)	UWB: Pozyx	ranges	ranges wrt static and moving agents
	embedded GNSS	positions	reference trajectory
	embedded camera	images	images
UAS2 (DJI Phantom 4Pro)	UWB: Pozyx	ranges	ranges wrt static and moving agents
	GNSS: Emlid M2	positions	reference trajectory
	embedded camera	images	images
UAS3 (DJI Phantom 4Pro)	UWB: Pozyx	ranges	ranges wrt static and moving agents
	GNSS: Emlid M2	positions	reference trajectory
	embedded camera	images, videos	images, videos
UAS4 (DJI Matrice 210)	UWB: Pozyx	ranges	ranges wrt static and moving agents
	embedded GNSS	positions	reference trajectory
	Camera: DJI FC6310S	Images, videos	images, videos
Car 0 (GPSVan)	UWB: Pozyx	ranges	ranges wrt static and moving agents
	GNSS: Leica GS25, Septentrio PolRx5	positions	reference trajectory from GNSS and IMU integration and correction
	IMU: Honeywell H764G	inertial information	
	LiDAR Velodyne VLP16	raw profiles	raw profiles with timestamp
Car 1 (Honda CRV)	UWB: Pozyx	ranges	ranges wrt static and moving agents
	GNSS: Topcon Hyper VR, Novatel PwrPak7	positions	reference trajectory from GNSS and IMU integration and correction
	IMU: SPAN-IGM-S1	inertial information	
	LiDAR Velodyne VLP16	raw profiles	raw profiles with timestamp
	Camera: Sony Alpha 6000	video	video
Car 2 (Honda Pilot)	UWB: Pozyx (anchor)	-	ranges wrt moving agents
	GNSS: 1 Topcon Hyper VR, 1 Novatel PwrPak7	positions	reference trajectory from GNSS and IMU integration and correction
	IMU: Epson G320 MEMS (built-in)	inertial information	
	LiDAR: Velodyne VLP16	raw profiles	raw profiles with timestamp
	Camera: GoPro HERO5	video	video
Car 3 (CyberCar)	UWB: Pozyx	ranges	ranges wrt static and moving agents
	GNSS: Topcon Hyper VR, Novatel PwrPak7	positions	reference trajectory from GNSS and IMU integration and correction
	IMU: Epson G320 MEMS (built-in)	inertial information	
	LiDAR: Velodyne VLP16	raw profiles	raw profiles with timestamp
	Camera: GoPro HERO5	video	video
Pedestrian 1	GNSS: Topcon Hyper VR	positions	reference trajectory
Pedestrian 2	GNSS: Topcon Hyper VR	positions	reference trajectory
Cyclist 1	GNSS: Topcon Hyper VR	positions	reference trajectory
Cyclist 2	GNSS: Topcon Hyper VR	positions	reference trajectory

Table 1: Summary of the platforms and sensors used during the data acquisition campaign, of the collected data and of those shared in the *CONTEST* dataset (available at https://github.com/3DOM-FBK/Collaborative_Navigation).

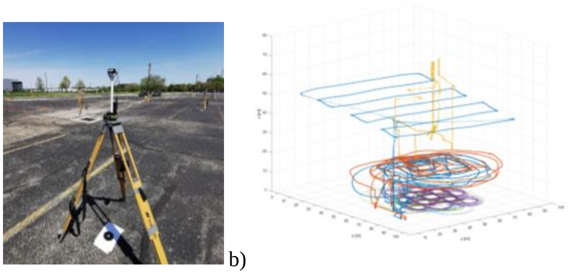
a) b)

Figure 3: Target and static UWB anchor for the V2I network (a). Reference GNSS-based trajectories of the four UASs and four ground vehicles (b).

The main objective of the field work was to acquire test data to support research on the integration of camera/LiDAR/UWB in a scalable collaborative positioning system involving both ground and aerial vehicles, representing a fairly unique 3D test scenario.

3.2 Ground truth data / control and reference solution

A key aspect of the campaign was to obtain highly accurate GNSS-based target locations and platform trajectory data, which can be used as reference and then for various simulation scenarios. The targets were GNSS-surveyed by RTK with 1-2 cm horizontal and 2-3 cm vertical accuracy. The ground platforms and drones primarily moved/flew predefined trajectories and rich sensor data was collected together with GNSS-based trajectories, see Fig.3b. The general pattern was to simulate traffic in a typical intersection area, where about 50% of traffic accidents happen.

3.3 Acquired data

Table 1 summarizes the platforms and sensors used during the data acquisition campaign and lists the data shared in the *CONTEST* dataset as well. Data are available for download at the following link:
https://github.com/3DOM-FBK/Collaborative_Navigation
Note that shared data have been created from raw data through some basic pre-processing and formatting operations, mostly aiming at improving the data usability.

4. DATA PROCESSING

Given the large variety of deployed platforms and sensors as well as the multiple data streams acquired, there are many scenarios where the performance of collaborative navigation can be tested and evaluated. First initial tests were performed to assess UWB-based collaborative navigation solutions for four ground vehicles.

4.1 UWB assessment

UWB ranging measurements were measured based on transceivers installed on ground vehicles and UASs as well as at the 12 targets. An example is shown in Fig. 4 which reports range measurements acquired for one and half hours by an UWB transceiver installed on a car. The horizontal lines indicate that there was no motion (no changes in the ranges). On the other hand, the areas with changing ranges represent three data collection sessions. In both static and moving states, there are outlier ranges, which can be filtered, for example, within a least squares estimation.
Fig. 5 shows an example of ranges collected by 4 cars and 4 UASs over a 40 s time interval. From the figure it is quite clear that ground vehicles collected more ranges, on average, with the only exception of Car2, which, differently from the others, was provided of an UWB anchor, hence it was only involved in V2V ranging.

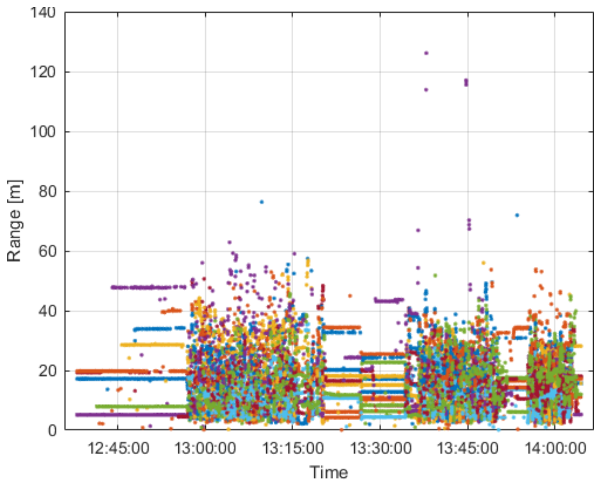

Figure 4: Range measurements (V2I and V2V) from UWB installed on a ground vehicle.

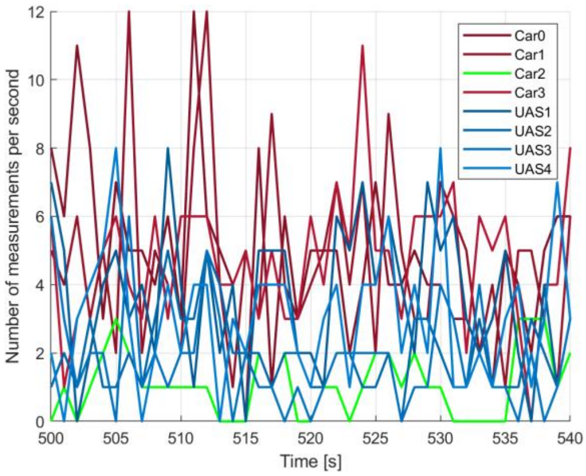

Figure 5: Range measurements of four cars and four UASs in a 40-s time interval.

Table 2 shows the distribution of the collected UWB ranges in terms of V2I and V2V measurements and, distinguishing whether the measurements where collected from ground vehicles to infrastructure (G2I), aerial platforms vs infrastructure (A2I), or, in the V2V case, among the different combinations of ground (G) and aerial (A) platforms.
Table 3 reports the UWB statistics for what concerns the 4 cars and 4 UASs on a 1500-s time interval (the first part of the test). A more comprehensive visualization of the number of measurements per second is shown in Fig. 6. Excluding Car 2, ground vehicles collected around 2.5 V2I ranges per second, whereas aerial platforms averaged only ~1 measurement per second. Instead, the average number of V2V ranges per second was approximately constant for all platforms (approximately 2).

Ranging category		**# of range meas. [%]**
V2I	**G2I**	42.7
	A2I	19.5
	V2I total	**62.2**
V2V	**G2G**	9.1
	A2A	9.5
	G2A	6.8
	A2G	12.4
	V2V total	**37.8**

Table 2: UWB ranging (percentage with respect to the total number of UWB measurements).

Platform	Mean	Std.dev.	Max
UAS1	2.4	1.9	12
UAS2	2.4	1.7	12
UAS3	3.4	2.5	14
UAS4	3.8	2.4	15
Car 0	4.7	2.5	15
Car 1	4.9	2.5	15
Car 2	1.4	1.2	8
Car 3	5.5	2.9	19

Table 3: UWB ranging statistics: number of measurements per second.

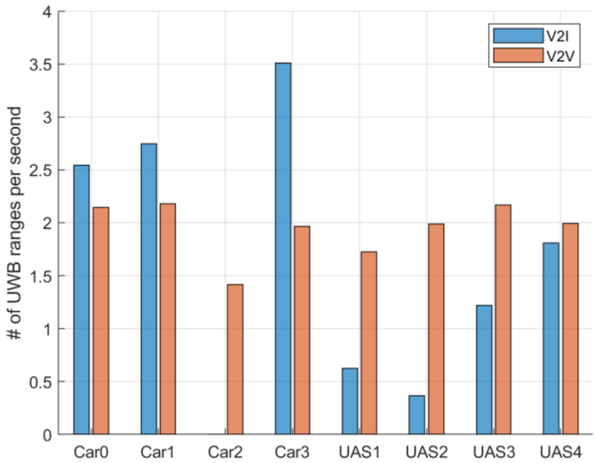

Figure 6: Comparison of the number V2I and V2V UWB measurements per second on the cars and UASs.

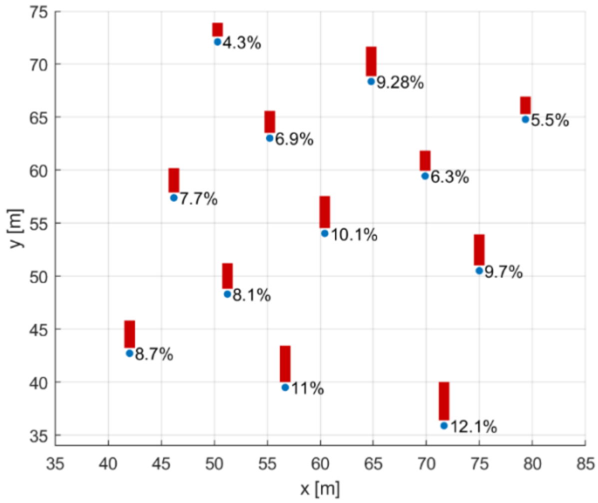

Figure 7: Distribution of the collected V2I ranges among the anchors.

While the V2V ranges are quite homogeneously distributed, the inhomogeneous distribution of the V2I shall be investigated more in depth. The distribution of the collected V2I ranges among the anchors is shown in Fig. 7. From Fig.7 it is quite clear that certain anchors have a much lower contribution to the collected ranges (e.g., the one on the top-left of the figure). However, according to the heat map of the ground vehicle locations, shown in Fig. 8, this is probably simply due to the fewer vehicle trajectories close to such anchors. Furthermore, the lower amount of V2I ranges for the aerial platforms with respect to the ground ones shall be explained by the average distance of such platforms from the anchors. Indeed, it is well known that the UWB ranging success rate decreases with the distance between the involved devices (Masiero et al., 2021) and, comparing the ground and aerial platform heat maps, shown in Figs. 8 and 9, respectively, it is quite clear that on average UASs flew at larger distances from the anchors than the ground vehicles. This is also confirmed by a comparison between UAS4 and the other UASs, as differently from the others, UAS4 flew at a higher altitude (~40 m from the ground vs ~20 m for the others) but at an almost constant horizontal location, approximately in the middle of the regions covered by the anchors (white spot approximately in the center of Fig. 9). This led to a higher V2I ranging success rate with respect to the other UASs, as shown in Figure 7.

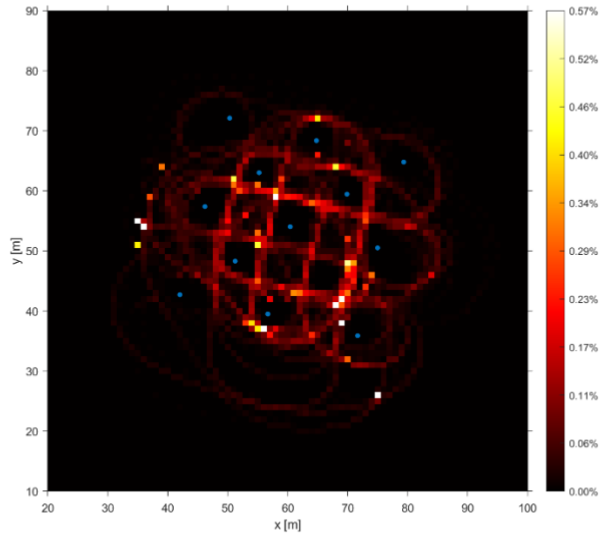

Figure 8: Heat map showing the common ground vehicle tracks during the first part of the test (1500-s time interval). Color visualization is saturated to the largest value in the color bar. UWB anchors are represented as blue disks.

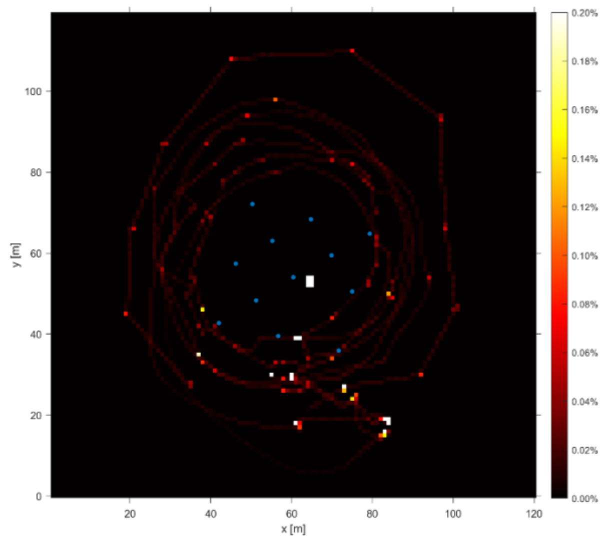

Figure 9: Heat map showing the common UAS tracks during the first part of the test (1500-s time interval). Color visualization is saturated to the largest value in the color bar. UWB anchors are represented as blue disks.

4.2 LiDAR data

Ground vehicles were provided of Velodyne VLP16 LiDARs, collecting up to 300K points per second. Azimuthal angular resolution was 0.2° during the tests.

Fig. 10 shows two views, oblique (a) and from the top (b), of a scene scanned by a Velodyne LiDAR mounted on Car 1. Fig. 10b clearly shows that, depending on where the LiDAR is mounted on the vehicle, a portion of the scene can be obstructed. Nevertheless, most of the time LiDAR can be used to detect the other vehicles/objects in the neighborhood of the sensor, e.g detected vehicles are shown with red boxes in Fig. 10b.

In addition to the possible obstructions, objects at longer distances are described by a lower number of points, hence reducing the chances of properly detecting them and determining their orientation. In accordance with this observation, Fig. 11 shows as an example the angular width distribution of vehicles from Car 1 in a 1500s long time interval.

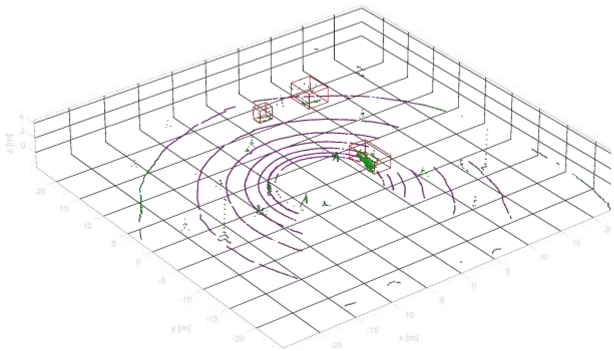

(a)

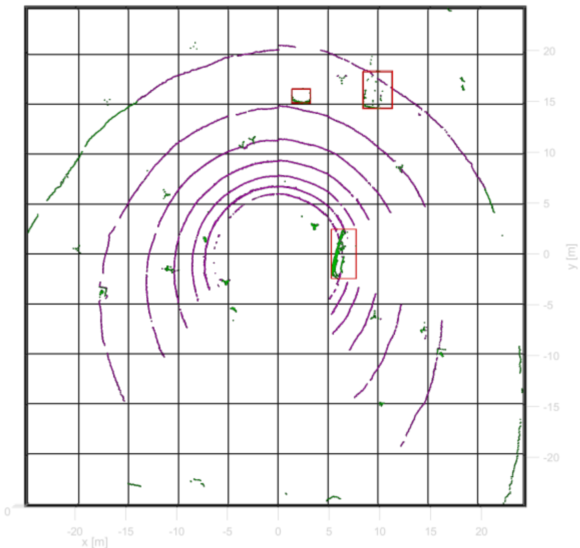

(b)

Figure 10: Example of oblique and top view of a LiDAR acquisition. The figure shows off-ground (green), ground points (violet) and the detected cars (red boxes).

4.3 UWB-based CN solution

The four ground vehicles were simultaneously moving in the considered area. UWB ranges were acquired between the vehicles (V2V) and, at the same time, all vehicles obtained range data with respect to the static UWB transceivers (V2I). Fig. 12 shows some localization solutions for a vehicle (Car 1) using the ranging and LiDAR data from the three other moving vehicles (Car 0, 2, 3) and from the anchor UWB transceivers. Black and red circles show the available (used) V2I and V2V UWB range measurements involving Car 1. Fig. 12a shows Car 1 outside of the UWB network, where despite the fact that there are six circles, they intersect at small angles, so the positioning accuracy is not good. Fig. 12b shows the vehicle along the boundary of the UWB network with only three circles and the three vehicles are inside, since they are almost along a line, so the accuracy is still not good. Fig. 12c shows a good case when all vehicles are inside the UWB network and there are six circles with several near perpendicular intersections, resulting in an accurate position.
These initial results, based only on UWB ranges for ground vehicles, show an acceptable solution for collaborative navigation. Further investigations on collaborative navigation tested on the *CONTEST* dataset will be considered in future works.

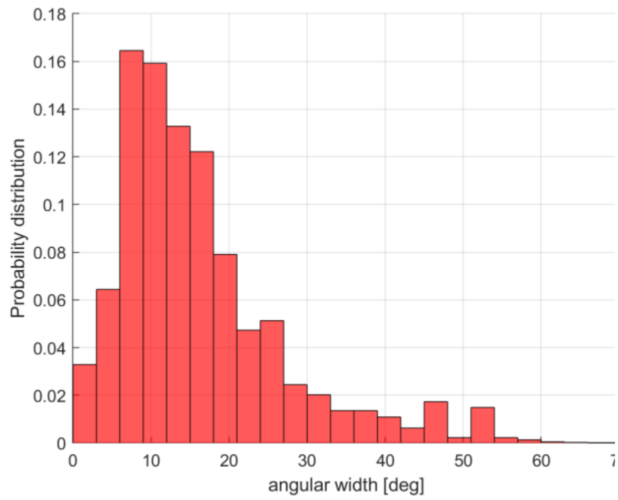

Figure 11: Angular width distribution of vehicles from Car 1 in a 1500s long time interval.

5. CONCLUSIONS

The development of an alternative positioning system, able to compensate unreliability and/or unavailability GNSS signal in certain scenarios (e.g. urban canyons and tunnels), can have remarkable positive impact on a large number of applications, for instance self-driving vehicles or indoor navigation, just to mention a few.

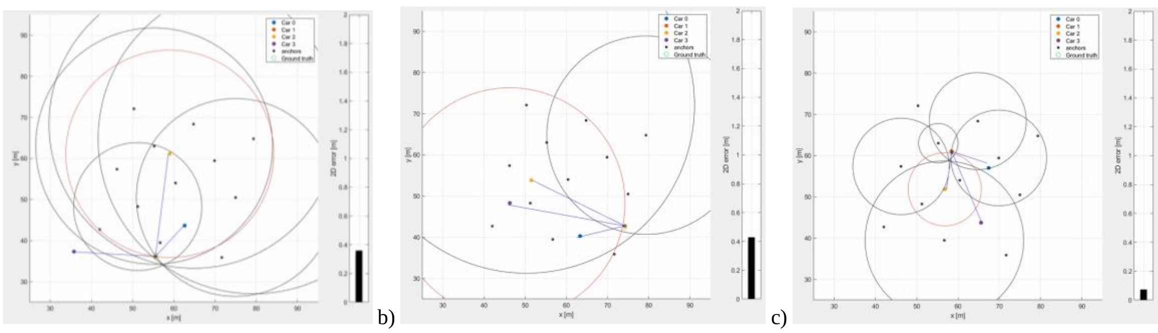

a) b) c)

Figure 12: UWB-based collaborative solution at different epochs. V2I and V2V UWB ranges involving Car 1 (red disk) are shown as circles, black and red, respectively. Blue segments show the positions of the vehicle positions as visible from LiDAR of Car 1.

An alternative positioning system shall be based on the integration of the information provided by different sensors, in order to ensure a robust and reliable solution in a wide variety of working conditions. In addition, exploiting information provided by other vehicles, in a collaborative approach, can be useful as well.
This paper presented a dataset, aiming at providing a common benchmark to research groups interested in this topic, and thus, support testing and comparative performance evaluation of the developed collaborative multi-sensor positioning approaches.
The presented benchmark dataset is based on measurements acquired from platforms that were jointly moving in 2D and 3D, which makes this benchmark unique and extremely useful. More specifically, the dataset contains data collected by both ground and aerial vehicles, acquiring reference (GNSS-based) trajectories, visual data, either as images or videos, LiDAR measurements and UWB ranges, both V2I and V2V.
In addition to a description of the data collection campaign and main characteristics of the dataset, some initial positioning and processing results are provided. A more comprehensive investigation on collaborative navigation using the collected dataset will be considered in future investigations.

ACKNOWLEDGEMENTS

This work was supported in part by the U.S. Department of Transportation under University Transportation Center Program Grant 69A3552047138.

REFERENCES

Bonenberg, L., Motella, B. and Fortuny Guasch, J., 2023. Assessing Alternative Positioning, Navigation and Timing Technologies for Potential Deployment in the EU. Publications Office of the European Union, Luxembourg, ISBN 978-92-68-01163-8, doi:10.2760/596229, JRC132737.

Buehrer, R. M., Wymeersch, H., Vaghefi, R.M., 2018. Collaborative Sensor Network Localization: Algorithms and Practical Issues. Proc. IEEE, 106(6), pp. 1089-1114.

Fan, S., Zhang, Y., Hao, Q., Jiang, P., Yu, C., Yu, F., 2019. Cooperative Positioning for Multi-AUVs Based on Factor Graph and Maximum Correntropy. IEEE Access 7, pp. 133327-133337.

Gabela, J., Retscher, R., Goel, S., Perakis, H., Masiero, A., Toth, Ch, Gikas, V., Kealy, A., Koppanyi, Z., Błaszczak-Bąk, V., Li, Yan., Grejner Brzezinska, D., 2019. Experimental Evaluation of a UWB-Based Cooperative Positioning System for Pedestrians in GNSS-Denied Environment. Sensors, Vol. 19, 5274.

Grejner-Brzezinska, D., C. Toth, T. Moore, J. Raquet, M. Miller, A. Kealy, 2016. Multi-sensor Navigation Systems: a Remedy for GNSS Vulnerabilities? Proceedings of the IEEE, Vol. 104, No. 6, pp. 1339-1353.

Humphreys, T., 2017. Interference. In: Springer Handbook of Global Navigation Satellite Systems. Ed. by P. Teunissen and O. Montenbruch. Springer. Chapter 16, pp. 469-304.

Kealy, A., Alam, N., Efatmaneshnik, M., Toth, C., Dempster, A., Brzezinska, D., 2016. Collaborative Positioning in GPS-Challenged Environments. Proc. IAG, Vol. 139.

Icking, L. and Schon, S., 2022. Optimal Combination of Multi-Agent Smartphone GNSS Observations for Improved Collaborative Positioning in Urban Areas. Proc. ION, pp. 2860-2870.

Ladai, A., C. Toth, 2022. Range-based Network Formation to Support Georeferencing Of Mapping Swarm Platforms, *Int. Arch. Photogramm. Remote Sens. Spatial Inf. Sci.*, XLVI-M-2-2022, 147–152..

Lee, J., Grejner-Brzezinska, D., Toth, C., 2012. Network-based Collaborative Navigation in GPS-Denied Environment. The Journal of Navigation, Vol. 63(3), pp. 443-437.

Liang, X., Milner, C., Macabiau, C., Estival, P., 2022. Multi-DMEs for alternative position, navigation and timing (A-PNT). The Journal of Navigation, 75(3), 625-645.

Masiero, A., Toth, Ch., Remondino, F., 2023. Vision and UWB-Based Collaborative Positioning Between Ground and UAS Platforms, 2023 *IEEE/ION Position, Location and Navigation Symposium (PLANS),* Monterey, CA, April 2023, pp. 748-754.

Masiero, A., Toth, C., Gabela, J., Retscher, G., Kealy, A., Perakis, H., Gikas, V., Grejner-Brzezinska, D., 2021. Experimental Assessment of UWB and Vision-Based Car Cooperative Positioning System. Remote Sensing, Vol. 13, 4858.

Menna, F., Torresani, A., Battisti, R., Nocerino, E., Remondino, F., 2022. A modular and low-cost portable VSLAM system for real-time 3D mapping: from indoor and outdoor spaces to underwater environments. Int. Arch. Photogramm. Remote Sens. Spatial Inf. Sci., XLVIII-2/W1-2022, pp. 153-162.

Mu, H., Bailey, T., Thompson, P., Durrant-Whyte, H., 2011. Decentralised Solutions to the Cooperative Multi-Platform Navigation Problem. Proc. IEEE Transactions on Aerospace and Electronic Systems, Vol. 47(2), pp. 1433-1449.

Pascacio, P., Casteleyn, S., Torres-Sospedra, J., Lohan, E., Nurmi, J., 2021. Collaborative Indoor Positioning Systems: A Systematic Review. Sensors, Vol. 21(3).

Raquet, J., 2013. Navigation using Pseudolites, Beacons, And Signals of Opportunity. NATO STO LectureSeries SET-197.

Ruegamer A., Kowalewski, D., 2015. Jamming and Spoofing of GNSS Signals – An Underestimated Risk?! Proc. FIG Cogress.

Schmidt, G.T., 2015. Navigation Sensors and Systems in GNSS Degraded and Denied Environments, Vol. 28(1).

Taketomi, T., Uchiyama, H., Ikeda, S., 2017. Visual SLAM algorithms: A survey from 2010 to 2016. IPSJ Transactions on Computer Vision and Applications, 9.1: 1-11.

Vitan, V., Berz, G., Saini, L., Arethens, J. P., Belabbas, B. and Hotmar, P., 2018. Research on Alternative Positioning Navigation and Timing in Europe. Proc. Integrated Communications, Navigation, Surveillance Conference (ICNS).

Wang, S. and Jiang, X., 2021. Three-Dimensional Cooperative Positioning in Vehicular Ad-hoc Networks. IEEE Transactions on Intelligent Transportation Systems, Vol. 22(2), pp. 937-930.

Wang, X., Toth, C., Grejner-Brzezinska, D., Masiero, A., 2022. Collaborative Navigation: Supporting PNT System Operational Anomaly Detection. Proc. IFAC International Symposium on Advances in Automotive Control, pp. 283-291.

Zidan, J., et al., 2016. GNSS Vulnerabilities and Existing Solutions: A Review of the Literature. IEEE Access, Vol. 9.

Zou, D., Tan, P., Yu, W., 2019. Collaborative visual SLAM for multiple agents: A brief survey. Virtual Reality & Intelligent Hardware, Vol. 1(3), pp. 461-482